Supplementary information

Investigations on a mononuclear Cu(II) Schiff base complex: Theoretical calculations, catechol oxidase activity, and protein binding interaction analysis

Bilash Chandra Roy,[a] Biswarup Dutta,[b] Dipmalya Basak,*[d] Surajit Debnath,*[c] Debashis Ray,*[b] and Tufan Singha Mahapatra*[a]

[a] *Department of Chemistry, Faculty of Science and Technology, ICFAI University Tripura, Agartala-799210, Tripura (W), India; E-mail: tufansmp@gmail.com, tsmahapatra@iutripura.edu.in*

[b] *Department of Chemistry, Indian Institute of Technology, Kharagpur 721 302, India E-mail: dray@chem.iitkgp.ac.in*

[c] *Department of Medical Laboratory Technology, Women's Polytechnic, Hapania Government of Tripura, Tripura, India; E-mail:drsurajitdebnathlab@gmail.com*

[d] *Department of Chemistry, National Institute of Technology Sikkim, Barfung Block, Ravangla Sub-Division, Dist. Namchi, Sikkim - 737 139, India; E-mail: basak.dipmalya@gmail.com*

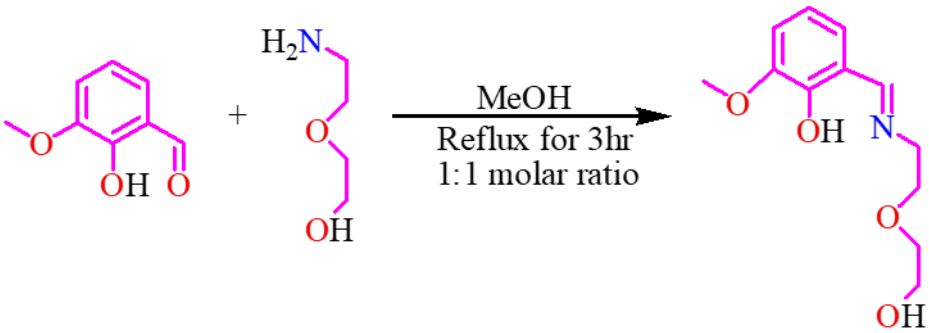

Scheme S1: Synthetic route of the preparation of H_2L Ligand.

Table S1: Crystallographic data and structural refinement of complex **1**.

Compound reference	Complex **1**
Chemical formula	$C_{24}H_{32}CuN_2O_8$
Formula Mass	540.07
Crystal system	Monoclinic
Space group	$P2_1/n$
Crystal color	Green
Crystal size/mm^3	0.26×0.20×0.15
a/Å	10.190(7)
b/Å	5.157(4)
c/Å	23.422(16)
α/°	90
β/°	102.01(2)

γ/°	90
V/Å^3	1203.9(14)
Z	2
D_c/g cm^{-3}	1.490
μ (mm^{-1})	0.959
F(000)	566
T/K	124(2)
Total reflns	15355
R(int)	0.0733
Unique reflns	2139
Observed reflns (I > 2σ(I))	1634
Parameters	195
R_1 (I > 2σ(I)), wR_2(all reflns)	0.0603, 0.1479
GOF (F^2)	1.056
Largest diff peak and hole (e Å^{-3})	0.914, -0.554
CCDC number	2141297

$R_1 = \Sigma(||F_o|-|F_c||)/\Sigma|F_o|$. $wR_2 = [\Sigma w(|F_o|-|F_c|)^2/\Sigma w(F_o)^2]^{1/2}$. $w = 0.75/(\sigma^2(F_o) + 0.0010F_o^2)$

Table S2: Selected bond lengths [Å] and bond angles [°] for complex **1**.

Complex1	
Distances	
Cu1-O1	1.884(3)
Cu1-N1	2.006(4)
Angles	
O1-Cu1-N1	88.19(14)
N1-Cu1-O1	88.20(14)
O1-Cu1-O1'	180.0(0)
N1-Cu1-N1'	180.0(2)

Table S3: Bond lengths (Å) and angles (°) for DFT optimized structures of H_2L.

Bond lengths (Å)		
	Gas phase	MeCN
C1-C2	1.4148	1.4141
C1-C6	1.384	1.3868
C1-H20	1.0936	1.0934
C2-C3	1.4186	1.4175
C2-C10	1.4575	1.461
C3-C4	1.4258	1.4232
C3-O9	1.329	1.3374
C4-C5	1.3947	1.3964
C4-O7	1.3566	1.3581
C5-C6	1.4099	1.4094
C5-H22	1.0907	1.0907
C6-H21	1.0928	1.0928
O7-C8	1.4064	1.4178
C8-H23	1.0986	1.098
C8-H24	1.1066	1.1042

C8-H25	1.1068	1.1044
O9-H18	1.0043	1.0133
C10-N11	1.2838	1.2837
C10-H26	1.1069	1.1054
N11-C12	1.4464	1.4498
C12-C13	1.5252	1.5235
C12-H27	1.1084	1.107
C12-H28	1.1039	1.1032
C13-O14	1.4131	1.4161
C13-H29	1.1114	1.1093
C13-H30	1.1034	1.1034
O14-C15	1.407	1.4158
C15-C16	1.5282	1.5251
C15-H31	1.1041	1.1038
C15-H32	1.1133	1.1098
C16-O17	1.4149	1.4191
C16-H33	1.1021	1.1028
C16-H34	1.1109	1.1091
O17-H19	0.9668	0.969
N11-H18	1.683	1.6479
Bond angles (°)		
	Gas phase	MeCN
C2-C1-C6	120.4392	120.2823
C2-C1-H20	118.885	118.9055
C1-C2-C3	120.0433	119.9433
C1-C2-C10	120.2556	120.3454
C6-C1-H20	120.6756	120.8121
C1-C6-C5	119.9106	120.108
C1-C6-H21	120.5802	120.5411
C3-C2-C10	119.7004	119.7113
C2-C3-C4	118.9521	119.2663
C2-C3-O9	122.419	121.9943
C2-C10-C11	122.661	122.0789
C2-C10-H26	116.5678	116.7865
C4-C3-O9	118.6288	118.7394
C3-C4-C5	119.707	119.6441
C3-C4-O7	115.0273	115.1621
C3-O9-H18	106.6445	106.0735
C5-C4-O7	125.2655	125.1938
C4-C5-C6	120.9474	120.7558
C4-C5-H22	119.9485	119.9971
C4-O7-C8	118.9118	118.7808
C6-C5-H22	119.1041	119.247
C5-C6-H21	119.5092	119.3509
O7-C8-H23	106.6259	106.4627
O7-C8-H24	112.0341	111.5831
O7-C8-H25	111.942	111.6082
H23-C8-H24	108.821	109.1405
H23-C8-H25	108.8235	109.1084
H24-C8-H25	108.5001	108.867
O9-H18-C11	149.0302	150.0351
N11-C10-H26	120.7712	121.1343
C10-N11-C12	119.9126	120.0773

C10-N11-H18	99.5345	100.1018
N11-C12-C13	111.3237	111.4783
N11-C12-H27	111.7831	111.4685
N11-C12-H28	108.9799	108.8547
C12-N11-H18	140.3945	139.7349
C13-C12-H27	108.5518	109.0024
C13-C12-H28	108.0144	107.7645
C12-C13-O14	108.0776	108.5762
C12-C13-H29	109.0959	108.8622
C12-C13-H30	110.2616	110.2673
H27-C12-H28	108.0643	108.146
O14-C13-H29	110.3458	110.4099
O14-C13-H30	111.2667	110.9765
C13-O14-C15	116.6789	115.8857
H29-C13-H30	107.7792	107.7277
O14-C15-C16	114.8795	114.4378
O14-C15-H31	106.1186	106.4654
O14-C15-H32	110.811	110.6146
C16-C15-H31	108.2244	107.9418
C16-C15-H32	109.4874	109.8139
C15-C16-O17	114.5216	114.5825
C15-C16-H33	108.5194	108.6829
C15-C16-H34	108.2929	108.0408
H31-C15-H32	106.9437	107.2351
O17-C16-H33	106.3517	106.4907
O17-C16-H34	111.5601	111.3519
C16-O17-H19	108.3852	107.9495
H33-C16-H34	107.3128	107.4364

Table S4: Calculated vibrational frequencies for H_2L.

Mode	Gas phase (cm^{-1})	MeCN (cm^{-1})	Mode	Gas phase (cm^{-1})	MeCN (cm^{-1})	Mode	Gas phase (cm^{-1})	MeCN (cm^{-1})
6	15.41	9.32	40	904.59	912.19	74	1462.13	1451.73
7	19.45	20.82	41	912.85	913.93	75	1465.07	1456.16
8	39.97	35.09	42	920.75	920.83	76	1469.12	1461.41
9	63	62.44	43	943.06	939.72	77	1476.53	1461.67
10	93.62	89.72	44	972.89	984.5	78	1480.12	1474.13
11	116.58	117.42	45	1002.49	989.61	79	1500.33	1487.59
12	128.52	129.17	46	1005.76	1006.19	80	1528.08	1510.36
13	157.97	153.99	47	1047.9	1043.91	81	1545.21	1542.95
14	165.08	163.45	48	1066.2	1064.44	82	1637.55	1629.31
15	205.98	202.61	49	1085.67	1080.28	83	1676.49	1671.51
16	239.59	233.72	50	1107.48	1100.97	84	1720.55	1712.94
17	252.15	243.53	51	1119.86	1108.49	85	2938.86	2865.31
18	266.13	263.33	52	1135.67	1121.46	86	2953.36	2971.71
19	310.03	305.43	53	1152.82	1144.28	87	2967.47	2977.17
20	315.79	324.86	54	1168.85	1163.46	88	2981.67	2984.52
21	335.1	337	55	1187.4	1164.41	89	2987.22	3001.89
22	352.81	349.53	56	1192.05	1176.11	90	3024.38	3004.73
23	362.01	358.28	57	1210.64	1203.2	91	3049.26	3049.69
24	367.75	365.89	58	1217.82	1221.97	92	3054.93	3066.1

25	391.94	394.54	59	1247.05	1243.34	93	3060.2	3067.79
26	431.28	432.21	60	1261.31	1257.67	94	3062.13	3075.47
27	500.51	501.07	61	1275.25	1273.89	95	3070.55	3080.15
28	515.72	515.37	62	1303.17	1288.87	96	3093.14	3083.36
29	550.48	550.92	63	1320.96	1313.78	97	3136.47	3147.89
30	576.09	573.55	64	1338.12	1316.13	98	3168.62	3174.88
31	583.14	581.28	65	1361.23	1355.92	99	3187.07	3190.36
32	602.29	601.76	66	1376.73	1375.67	100	3209.51	3214.2
33	632.41	630.21	67	1386.65	1380.04	101	3801.57	3779.85
34	744.75	740.77	68	1390.41	1385.82			
35	745.17	743.06	69	1403.92	1396.52			
36	787.2	788.19	70	1412.19	1409.49			
37	820.98	819.98	71	1420.64	1414.64			
38	857.21	852.21	72	1459.34	1449.37			
39	898.34	894.67	73	1461.75	1450.95			

Table S5: Calculated vibrational frequencies for $Cu(HL)_2$.

Mode	Sq.Pl. Gas phase (cm^{-1})	Dist.Sq.Pl. MeCN (cm^{-1})	Mode	Sq. Pl. Gas phase (cm^{-1})	Dist.Sq.Pl. MeCN (cm^{-1})	Mode	Sq. Pl. Gas phase (cm^{-1})	Dist.Sq.Pl. MeCN (cm^{-1})
6	6.05	6.94	71	754.85	750.91	136	1383.61	1378.46
7	17.31	12.62	72	754.86	752.86	137	1403.43	1394.59
8	19.08	17.31	73	755.4	754.5	138	1405.99	1396.83
9	19.41	20.48	74	757.76	755.19	139	1416.61	1409.85
10	22.91	21.7	75	799.91	795.73	140	1416.66	1413.05
11	28.73	26.73	76	800.79	796.64	141	1429.25	1420.34
12	34.1	32.68	77	844.89	839.54	142	1430.13	1423.71
13	41.91	39.76	78	845.61	840.74	143	1441.82	1436.34
14	47.65	46.56	79	877.38	872.01	144	1441.9	1437.45
15	53.42	49.18	80	878.6	872.1	145	1455.12	1444.59
16	68.57	56.26	81	904.06	905.67	146	1460.37	1447.46
17	73.24	85.33	82	904.07	906.95	147	1462.68	1449.22
18	89.69	87.2	83	908.58	911.38	148	1462.7	1451.02
19	93.3	89.63	84	909.16	911.58	149	1468.34	1460.53
20	111.71	107.93	85	932.74	925.19	150	1468.79	1461.44
21	116.17	116.64	86	933.72	927.99	151	1476.38	1464.32
22	120.23	119.72	87	938.61	933.64	152	1476.39	1466.09
23	127.32	125.1	88	938.87	934.6	153	1480.92	1466.94
24	136.52	131.88	89	974.25	981.43	154	1480.99	1467.05
25	144.95	143.36	90	974.29	983.06	155	1481.49	1468.16
26	165.06	161.35	91	1004.45	999.14	156	1481.49	1472.64
27	166.75	166.86	92	1004.57	999.96	157	1491.12	1481.68
28	175.71	173.75	93	1016.75	1008.7	158	1492.22	1484.64
29	182.85	177.9	94	1017.12	1012.28	159	1501.66	1490.39
30	182.95	182.16	95	1073.15	1065.72	160	1501.9	1494.23
31	202.49	197.54	96	1073.46	1069.13	161	1518.79	1505.59
32	210.9	212.9	97	1085.78	1079.1	162	1522.44	1507.17
33	217.74	218.79	98	1085.84	1079.42	163	1600.15	1589.99
34	247.83	242.46	99	1101.41	1089.36	164	1600.85	1591.08
35	252.96	249.56	100	1102.01	1089.52	165	1655.06	1646.13

36	263.53	257.55	101	1111.84	1101.99	166	1655.99	1647.43
37	265.31	261.05	102	1112.09	1102.57	167	1683.93	1673.75
38	292.85	286.58	103	1120.64	1111.51	168	1688.89	1679.7
39	299.28	296.11	104	1120.67	1112.13	169	2960.93	2972.1
40	314.88	308.33	105	1145.25	1130.83	170	2960.94	2975.97
41	321.91	317.46	106	1145.57	1131.68	171	2965.57	2980.1
42	332.08	322.11	107	1155.14	1145.18	172	2965.62	2983.11
43	337.95	328.33	108	1156.34	1145.99	173	2977.75	2985.62
44	343.34	334.44	109	1172.18	1159.39	174	2977.87	2990.74
45	360.14	353.59	110	1172.18	1162.61	175	2987.17	2998.64
46	365.93	361.54	111	1176.32	1166.83	176	2987.32	3002.14
47	366.18	364.35	112	1177.07	1169.13	177	3011.27	3014.25
48	379.52	373.9	113	1190.22	1177.92	178	3011.29	3022.19
49	382.93	378.73	114	1190.37	1179.41	179	3024.79	3026.03
50	395.87	392.64	115	1213.5	1203.55	180	3025.03	3033.62
51	429.74	406.41	116	1213.7	1203.9	181	3052.21	3034.23
52	445.6	408.04	117	1234.08	1226.63	182	3052.23	3070.46
53	460.89	428.3	118	1234.09	1232.09	183	3056.32	3073.37
54	461.46	441.02	119	1246.86	1245.5	184	3056.35	3076.62
55	480.07	467	120	1248.96	1247.8	185	3073.96	3081.43
56	481.16	474.62	121	1255.58	1251.91	186	3074.38	3086.94
57	537.71	536.91	122	1258.78	1253.73	187	3079.47	3090.56
58	539.89	539.57	123	1268.17	1259.4	188	3079.48	3091.84
59	540.35	541.91	124	1268.3	1261.18	189	3133.2	3133.87
60	543.32	543.14	125	1285.65	1274.25	190	3133.22	3139.13
61	563.33	560.87	126	1287.82	1275.53	191	3152.74	3145.3
62	566.03	564.48	127	1297.58	1286.83	192	3152.79	3145.77
63	566.81	566.29	128	1300.43	1289.57	193	3168.96	3165.85
64	573.46	570.17	129	1368.07	1358.55	194	3169.01	3173.3
65	596.97	597.14	130	1368.3	1363.53	195	3191.52	3189.73
66	597.18	597.89	131	1377.81	1365.75	196	3191.54	3191.69
67	612.59	608.74	132	1378.95	1368.08	197	3207.01	3208.37
68	631.88	623.65	133	1379.26	1370.18	198	3207.05	3208.99
69	638.55	634.89	134	1380.92	1371.54	199	3788.75	3767.19
70	641.26	637.24	135	1383.09	1377.33	200	3788.82	3768.63

Table S6: Various peaks in the calculated and experimental electronic spectra of H_2L including the main contributing electronic transition states.

TD-DFT Calculated (nm)		Experimental (nm)/MeCN	Electronic transition state/MeCN
Gas phase	MeCN		
208.74	209.25	222	S7 (E = 5.939 eV)
–	232.57	251.50	S6 (E = 5.327 eV)
245.81	247.93	263.50	S4 (E = 4.999 eV)
–	311.54	299	S2 (E = 3.978 eV)
321.63	331.71	329.50	S1 (E = 3.739 eV)

Table S7: Comparison of bond distances (Å) and angles (°) for optimized structures with Sq.Pl. and Dist.Sq.Pl. geometry around metal center.

Bond lengths (Å)		
	Sq.Pl.	Dist.Sq.Pl.
N3-Cu1	2.0316	2.0146

N36-Cu1	2.0316	2.0133
O2-Cu1	1.9156	1.9259
O35-Cu1	1.9156	1.9243
Bond angles (°)		
	Sq.Pl.	Dist.Sq.Pl.
N3-Cu1-O35	88.1518	91.9027
N3-Cu1-O2	91.8482	91.8681
N36-Cu1-O35	91.8482	91.9837
N36-Cu1-O2	88.1518	91.3897
N3-Cu1-N36	179.9744	160.7931
O35-Cu1-O2	179.9744	158.4611

Table S8: Various peaks in the calculated and experimental electronic spectra of $Cu(HL)_2$ including the main contributing electronic transition states.

TD-DFT Calculated (nm)/MeCN		Experimental (nm)/MeCN	Electronic transition state/Dist.Sq.Pl.
Sq.Pl.	Dist.Sq.Pl.		
278.04	296.97	241	S29 (E = 4.222 eV)
331.73	338.48	278.50	S21 (E = 3.733 eV)
353.20	355.78	305	S17 (E = 3.446 eV)
–	461.28	370	S8 (E = 2.691 eV)
–	524.13	484.50	S4 (E = 2.368 eV)
–	657.88	646	S2 (E = 1.885 eV)
–	846.41	959	S1 (E = 1.464 eV)

CASSCF Calculated (nm)/MeCN		Experimental (nm)/MeCN	Calculated Roots and Electronic transition state
Sq.Pl.	Dist.Sq.Pl.		
–	991	959	Dist.Sq.Pl. Root 0: $d_{z^2}(2), d_{xz}(2), d_{yz}(2), d_{xy}(2), d_{x^2-y^2}(1)$; 95.489% Root 1: $d_{z^2}(2), d_{xz}(2), d_{yz}(2), d_{xy}(1), d_{x^2-y^2}(2)$; 95.440% Electronic transition state: 0→1 (1.251 eV) Sq.Pl. Root 0: $d_{z^2}(2), d_{xz}(2), d_{yz}(2), d_{xy}(2), d_{x^2-y^2}(1)$; 99.304% Root 1: $d_{z^2}(2), d_{xz}(2), d_{yz}(2), d_{xy}(1), d_{x^2-y^2}(2)$; 99.296% Electronic transition state: 0→1 (1.347 eV)

Table S9: CASSCF calculated ligand field one electron eigenfunctions for optimized structure having Dist.Sq.Pl. geometry around metal center.

Orbital	Energy (eV)	d_{xy}	d_{yz}	d_{z^2}	d_{xz}	$d_{x^2-y^2}$
1	0	0.030685	0.291114	0.918117	-0.26531	0.031388
2	0.044	-0.20994	0.865637	-0.3445	-0.27861	-0.10146
3	0.195	0.01511	-0.33382	-0.16396	-0.91082	0.178482
4	0.318	-0.97694	-0.17915	0.099563	0.040232	0.044409
5	1.569	0.018854	0.149643	-0.03984	0.144126	0.977186

Table S10: CASSCF calculated ligand field one electron eigenfunctions for optimized structure having Sq.Pl. geometry around metal center.

Orbital	Energy (eV)	d_{xy}	d_{yz}	d_{z^2}	d_{xz}	$d_{x^2-y^2}$
1	0	0	-0.00368	0.605058	-0.76952	0.199418
2	0.003	25.5	0.081049	-0.77005	-0.62692	-0.08475
3	0.157	1262.9	-0.00405	-0.19189	0.105201	0.973563
4	0.354	2855.1	0.996472	0.064102	0.047771	0.013085
5	1.701	13719.4	-0.02108	0.000784	-0.03823	0.071089

Table S11: Comparision of k_{cat} values of complex **1** with other reported complexes in literature

Complex	**k_{cat}, h^{-1}**	**Reference**
$[Cu^{II}(H_2LDA)(ClO_4)](ClO_4)$	58.68	1
[Cu(**L1**)Cl_2]	5.1×10^5	2
$[Cu^{II}(HL)_2]$	2.64×10^3	3
[Cu(pymimi)Cl_2] [Cu(pymima)Cl_2]	216 396	3
$[CuL(NO_3)(H_2O)]\cdot(H_2O)$	$1.45X10^4$	4
[Cu(L)(N_3)]	898	5
$[Cu^{II}$(sal-ppzH)$Cl_2]$ $[Cu^{II}$(hyap-ppzH)$Cl_2]$	1.970×10^2 4.801×10^2	6
$[Cu(L^1)](ClO_4)_2$ $[Cu(L^2)](ClO_4)_2$	9.72 $12.24X10^{-2}$	7
$[Cu(HL)_2]$ (1)	**19.87**	**Present Work**

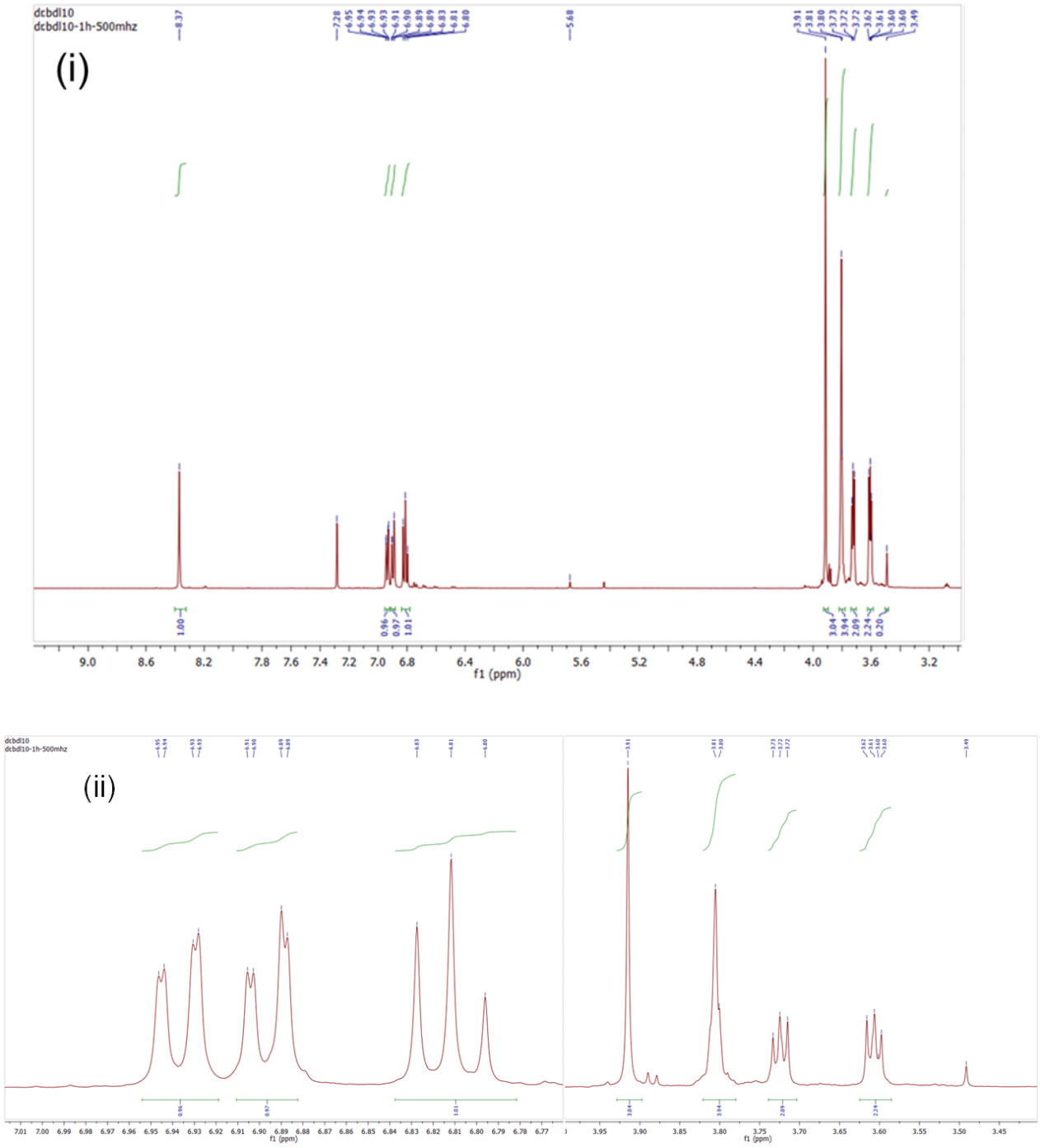

Fig. S1: ^{1}H NMR of H_2L ligand in $CDCl_3$.(i) Full spectrum (ii) Expanded on aromatic and aliphatic portions.

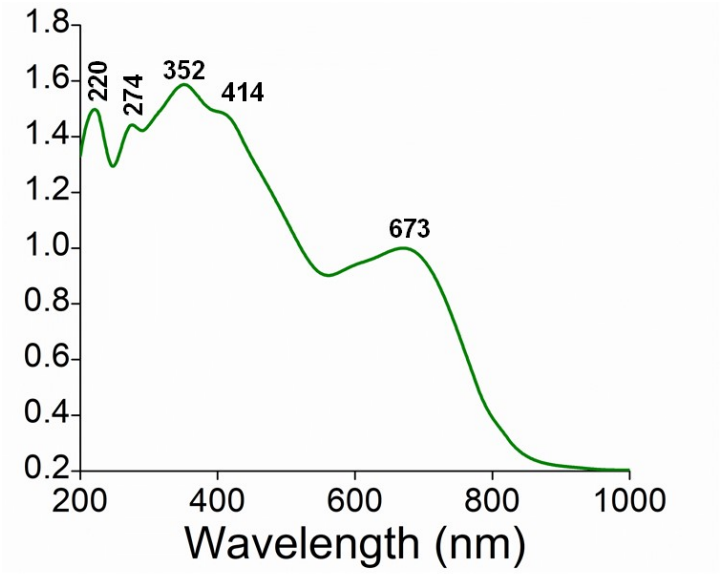

Fig. S2: The diffuse-reflectance spectra of complex **1.**

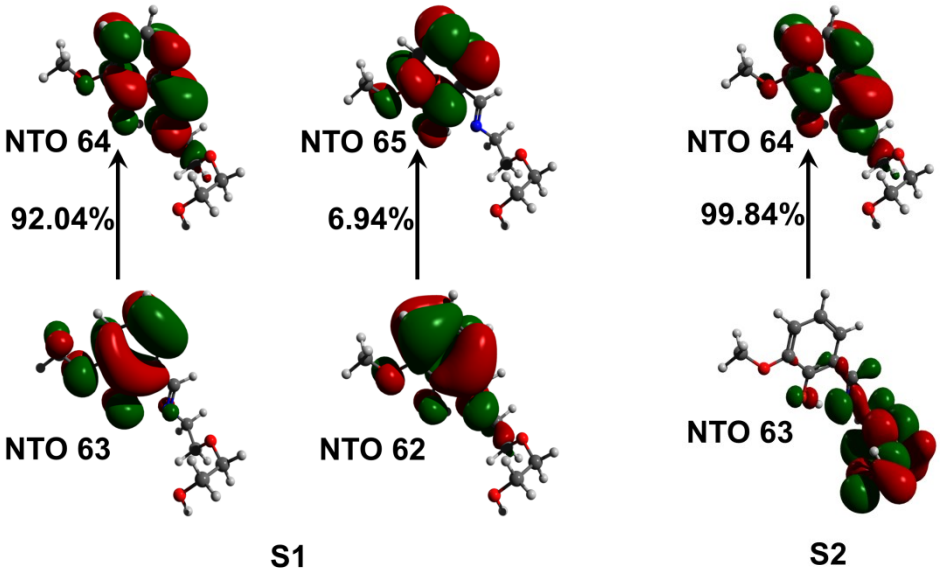

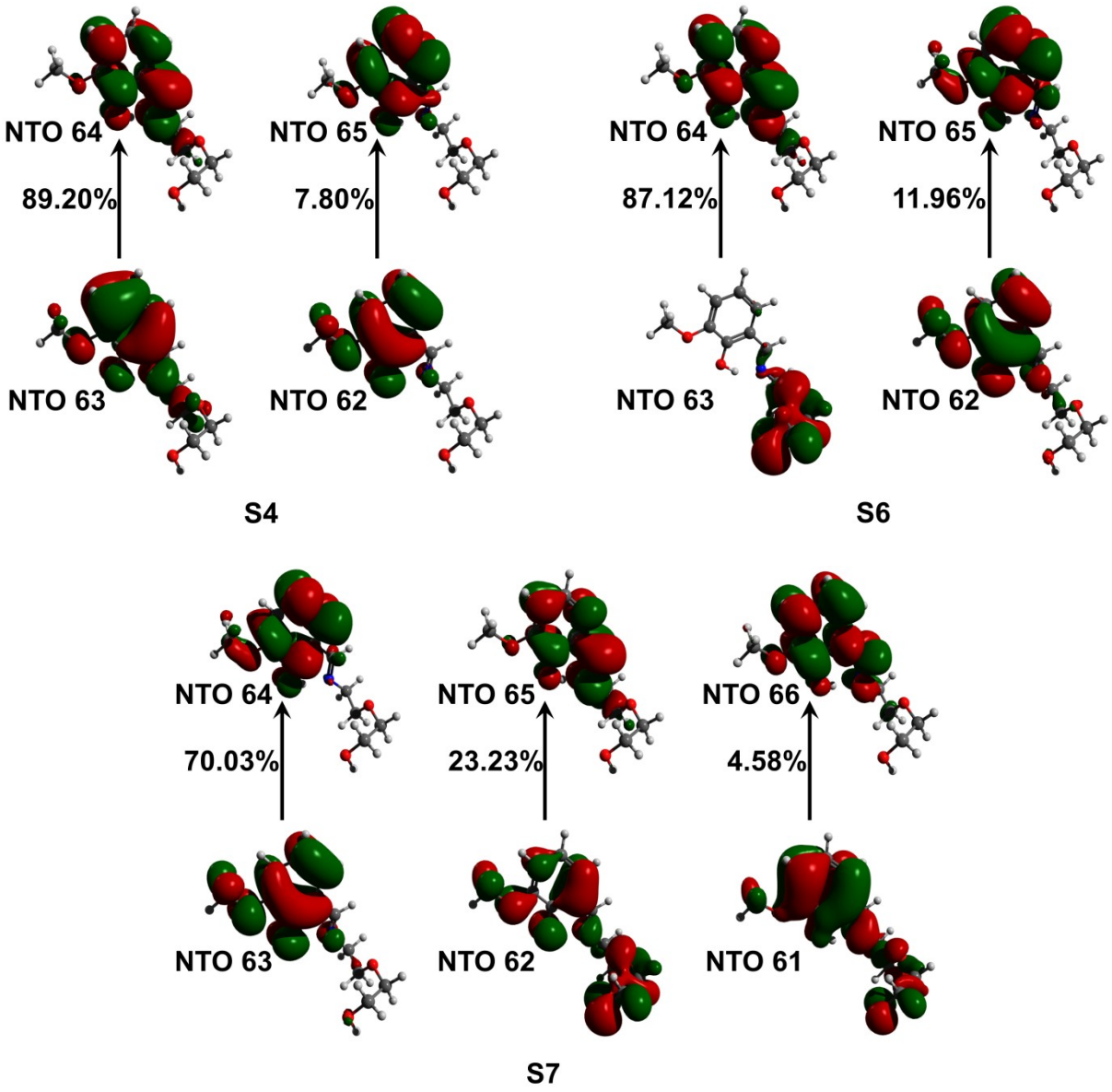

Fig. S3: Major contributing NTOs for the main electronic transition states responsible for the TD–DFT calculated electronic spectra of H_2L in MeCN.

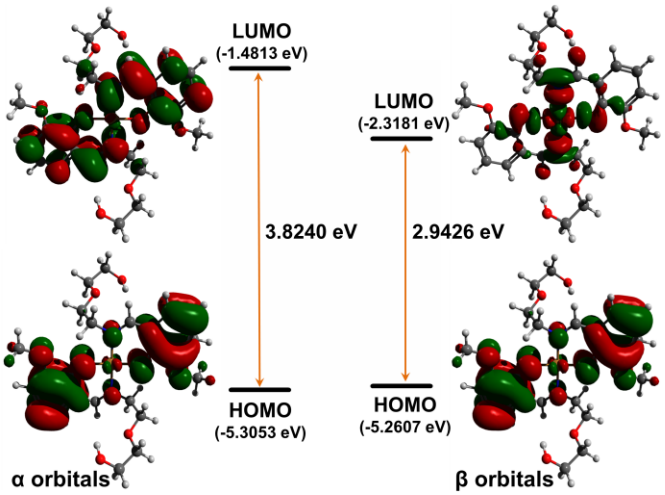

Fig. S4: HOMO–LUMO gap for $Cu(HL)_2$ considering Sq.Pl. geometry around Cu(II) in MeCN.

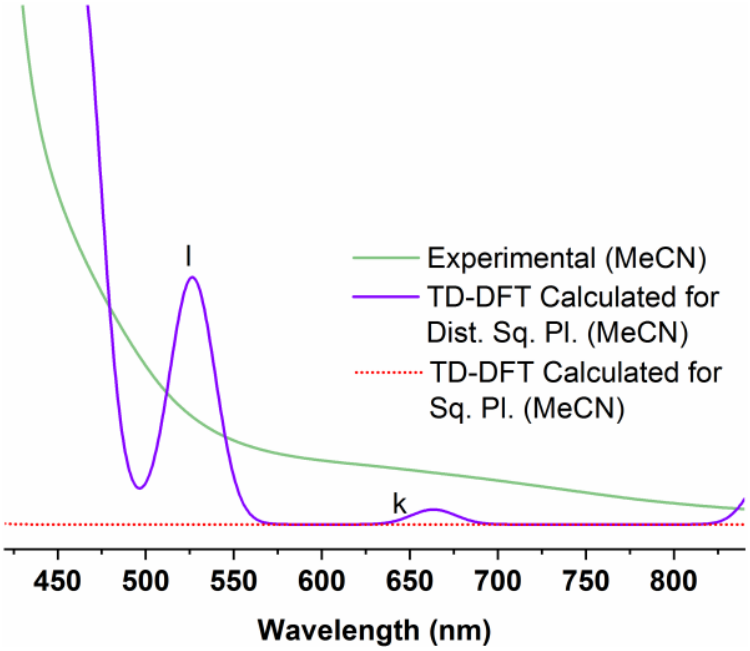

Fig. S5: Calculated and experimental UV–vis spectra of $Cu(HL)_2$. Here, k: 88.01% HOMO-1 β → LUMO β; l: 28.32% HOMO-10 β → LUMO β, 17.86% HOMO-2 β → LUMO β.

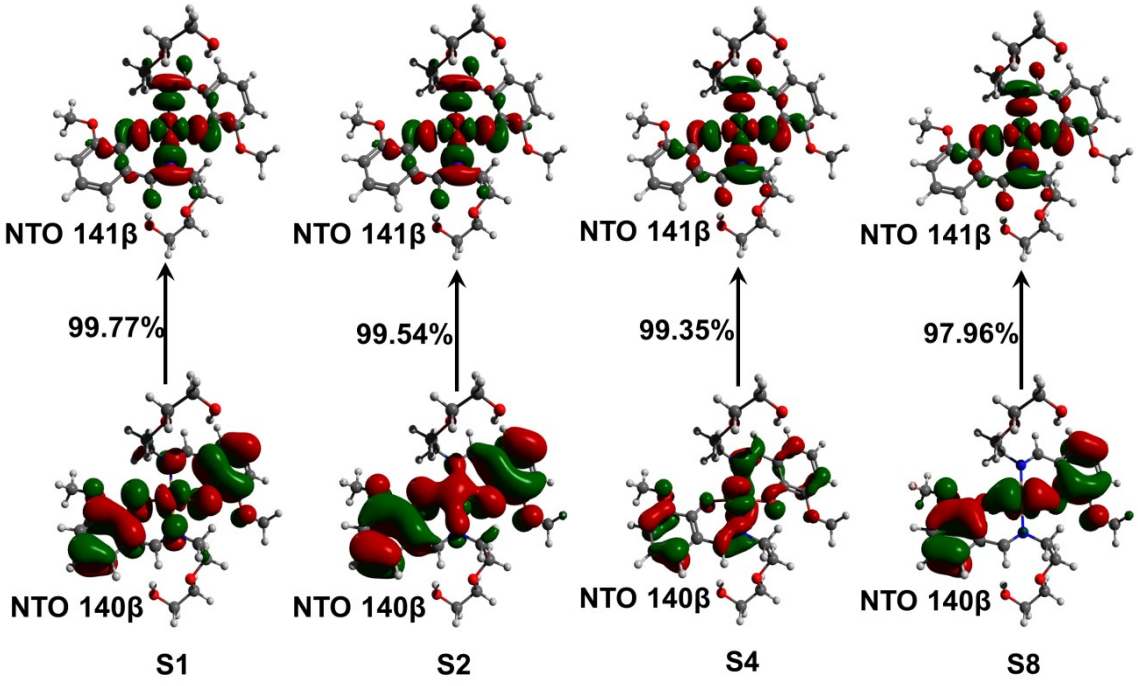

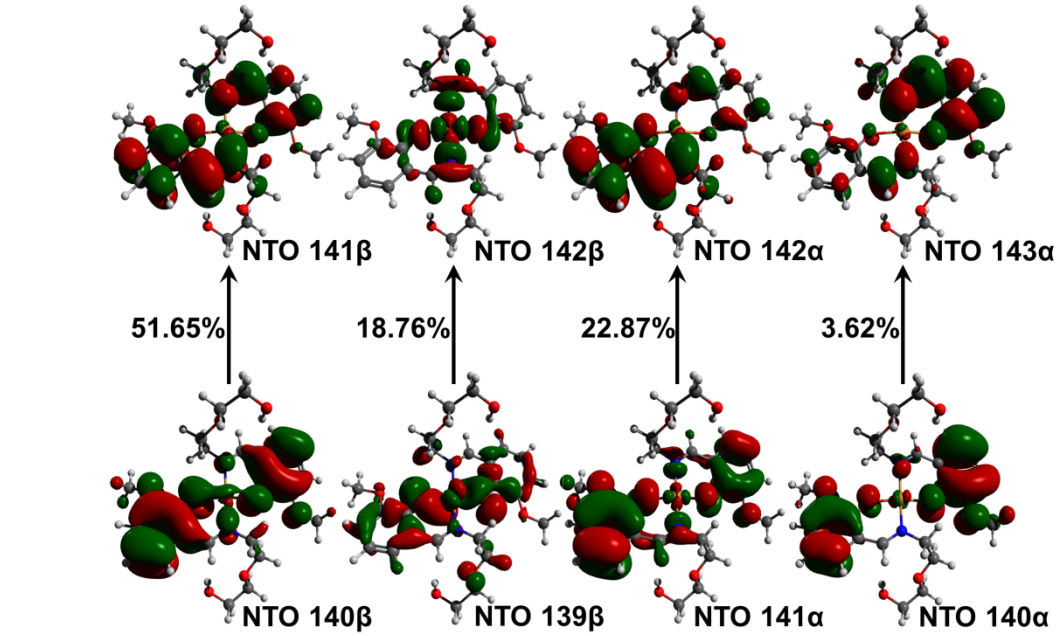
NTO 141β
NTO 142β
NTO 142α
NTO 143α
51.65%
18.76%
22.87%
3.62%
NTO 140β
NTO 139β
NTO 141α
NTO 140α

S17

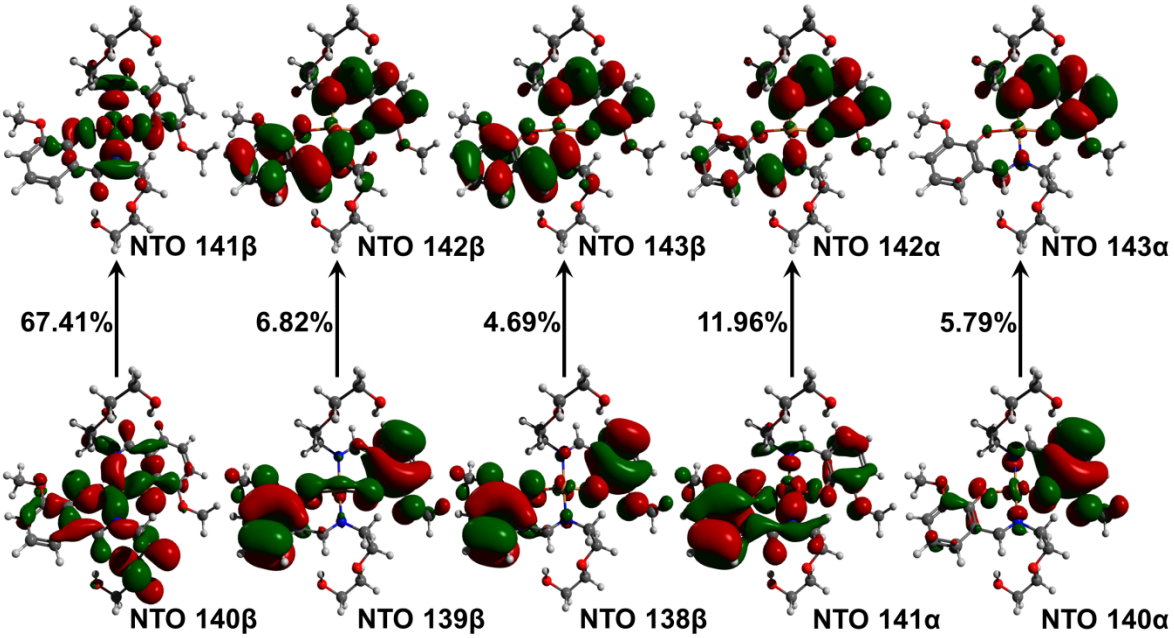
NTO 141β
NTO 142β
NTO 143β
NTO 142α
NTO 143α
67.41%
6.82%
4.69%
11.96%
5.79%
NTO 140β
NTO 139β
NTO 138β
NTO 141α
NTO 140α

S21

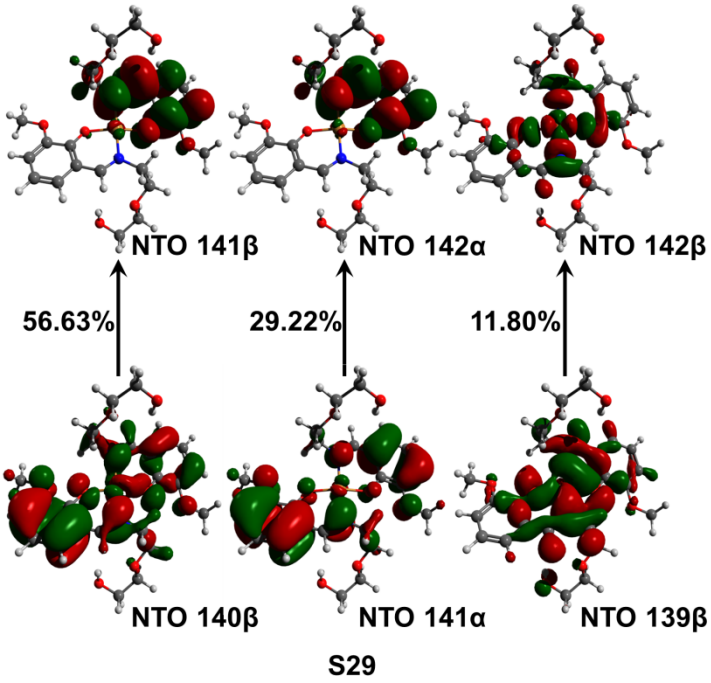

Fig. S6: Major contributing NTOs for the main electronic transition states responsible for the TD–DFT calculated electronic spectra of $Cu(HL)_2$ in MeCN.

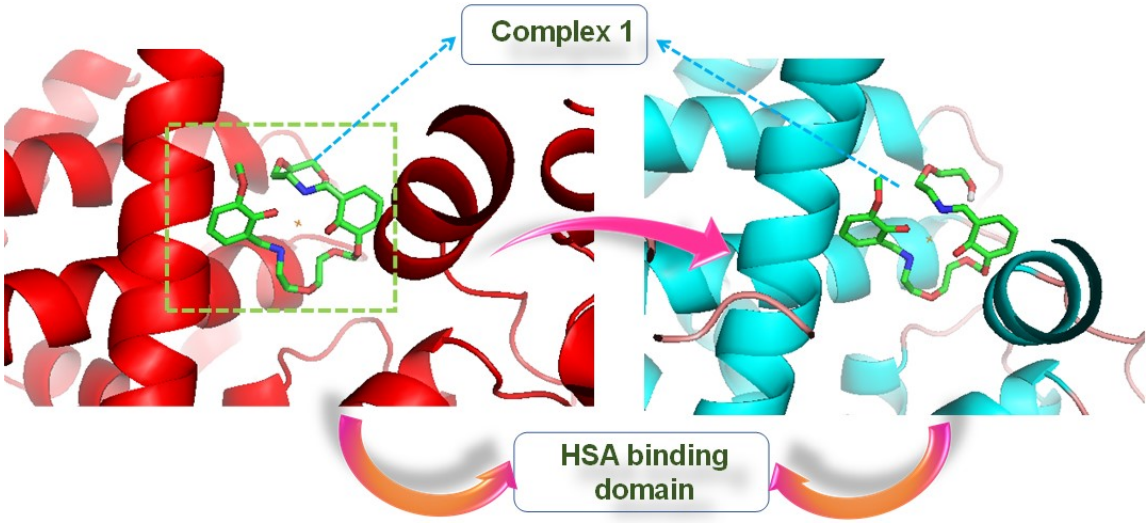

Fig. S7: Complex **1** binding with HSA polypeptide.

References:

1 T. P. Camargo, R. A. Peralta, R. Moreira, E. E. Castellano, A. J. Bortoluzzi and A. Neves, *Inorganic Chemistry Communications*, 2013, **37**, 34-38.

2 R. Maity, M. Maity, K. Jana, T. Maity, N. Sepay and B. C. Samanta, *New Journal of Chemistry*, 2023, **47**, 2673-2681.

3 M. Mitra, A. K. Maji, B. K. Ghosh, G. Kaur, A. Roy Choudhury, C.-H. Lin, J. Ribas and R. Ghosh, *Polyhedron*, 2013, **61**, 15-19.

4 S. Anbu, A. Paul, A. P. C. Ribeiro, M. F. C. Guedes da Silva, M. L. Kuznetsov and A. J. L. Pombeiro, *Inorganica Chimica Acta*, 2016, **450**, 426-436.

5 S. Mondal, M. Chakraborty, A. Mondal, B. Pakhira, A. J. Blake, E. Sinn and S. K. Chattopadhyay, *New Journal of Chemistry*, 2018, **42**, 9588-9597.

6 S. Kumari, A. K. Mahato, A. Maurya, V. K. Singh, N. Kesharwani, P. Kachhap, I. O. Koshevoy and C. Haldar, *New Journal of Chemistry*, 2017, **41**, 13625-13646.

7 J. L. Viegas and S. N. Dhuri, *Journal of Molecular Structure*, 2023, DOI: https://doi.org/10.1016/j.molstruc.2023.135719, 135719.

----------Thanks----------